Foxp2 Regulates Identities and Projection Patterns of Thalamic Nuclei during Development

Foxp2 regulates identities and projection patterns of thalamic nuclei during development

Haruka Ebisu[1,2,3,4], Lena Iwai-Takekoshi[4], Eriko Fujita-Jimbo[5], Takashi Momoi[6], and Hiroshi Kawasaki[1,2,4]

[1] Department of Medical Neuroscience, Graduate School of Medical Sciences, Kanazawa University, Ishikawa 920-8640, Japan
[2] Brain/Liver Interface Medicine Research Center, Kanazawa University, Ishikawa 920-8640, Japan
[3] Department of Neurology, Graduate School of Medicine, The University of Tokyo, Tokyo 113-0033, Japan
[4] Department of Molecular and Systems Neurobiology, Graduate School of Medicine, The University of Tokyo, Tokyo 113-0033, Japan
[5] Department of Pediatrics, Jichi Medical University, Tochigi 329-0498, Japan
[6] Department of Pathophysiology, Tokyo Medical University, Tokyo 160-8402, Japan

Running Title: Foxp2 in thalamic patterning

Address correspondence to
Hiroshi Kawasaki, MD, PhD
Department of Medical Neuroscience
Graduate School of Medical Sciences
Kanazawa University
Takara-machi 13-1, Kanazawa, Ishikawa 920-8640, Japan
Tel: +81-76-265-2363
Fax: +81-76-234-4274
E-mail: hiroshi-kawasaki@umin.ac.jp

Abstract

The molecular mechanisms underlying the formation of the thalamus during development have been investigated intensively. Although transcription factors distinguishing the thalamic primordium from adjacent brain structures have been uncovered, those involved in patterning inside the thalamus are largely unclear. Here we show that Foxp2, a member of the forkhead transcription factor family, regulates thalamic patterning during development. We found a graded expression pattern of Foxp2 in the thalamic primordium of the mouse embryo. The expression levels of Foxp2 were high in the posterior region and low in the anterior region of the thalamic primordium. In Foxp2 (R552H) knockin mice, which have a missense loss-of-function mutation in the forkhead domain of Foxp2, thalamic nuclei of the posterior region of the thalamus were shrunken, while those of the intermediate region were expanded. Consistently, Foxp2 (R552H) knockin mice showed changes in thalamocortical projection patterns. Our results uncovered important roles of Foxp2 in thalamic patterning and thalamocortical projections during development.

Key words: Foxp2, thalamic patterning

Introduction

The thalamus plays critical roles as a relay center of sensory information in the brain. Most sensory information is transmitted from the periphery to the primary sensory areas in the cerebral cortex through the thalamus, and the loss of thalamic functions results in severe sensory deficits (Jones 2007). The thalamus consists of many structurally and functionally segregated nuclei, which are thought to be structural bases of sensory information processing in the thalamus. For example, the ventral posterior nucleus (VP) of the thalamus conveys somatosensory information and sends its axons to the primary somatosensory area (S1) of the cerebral cortex.

Early in development, the thalamic primordium is distinguished from adjacent brain structures such as the prethalamus, the pretectum and the epithalamus. Then, the thalamic primordium differentiates into various thalamic nuclei such as the anterodorsal nucleus (AD), the anteroventral nucleus (AV), the posterior nucleus (Po) and the VP. This process leading to the formation of thalamic nuclei is called thalamic patterning. The AD and the AV are located in the anterior region of the thalamus, whereas the VP and the Po reside in the posterior region.

The mechanisms that distinguish the thalamic primordium from adjacent brain structures have been extensively examined (Kiecker and Lumsden 2012). Previous papers have uncovered transcription factors regulating the formation of the thalamic primordium (Kobayashi et al. 2002; Braun et al. 2003; Hirata et al. 2006; Puelles et al. 2006; Peukert et al. 2011; Bluske et al. 2012; Robertshaw et al. 2013; Chatterjee et al. 2014). The homeodomain transcription factor Otx2 is required for acquiring thalamic identity, and the lack of Otx2 results in the activation of markers of the pretectum (Puelles et al. 2006). The zinc finger transcription factors Fezf1 and Fezf2 are crucial for the formation of the prethalamus and the thalamus (Hirata et al. 2006). Irx3 and Pax6 are involved in creating the cellular competence necessary for the formation of the

thalamus (Robertshaw et al. 2013). In contrast, transcription factors regulating patterning inside the thalamus are still largely unclear, even though recent pioneering studies uncovered several molecules expressed in specific subsets of thalamic nuclei (Nakagawa and O'Leary 2001, 2003; Jones and Rubenstein 2004; Yuge et al. 2010). In this study, we focus on the transcriptional factor Foxp2, which is a member of the forkhead transcription factor family. The forkhead transcription factor family consists of more than 30 transcription factors, many of which play crucial roles in developmental processes and in the pathophysiology of diseases (Lehmann et al. 2003; Fujita et al. 2008; Enard et al. 2009; Fisher and Scharff 2009; Hannenhalli and Kaestner 2009; French et al. 2012). We demonstrate that Foxp2 regulates thalamic patterning and thalamocortical projection during development.

Materials and Methods

Animals

ICR mice (*Mus musculus*) were purchased from SLC (Hamamatsu, Japan) and were reared on a normal 12 hr light/dark schedule. The day of insemination was designated as embryonic day 0 (E0), and the day of birth was defined as postnatal day 0 (P0). Foxp2 (R552H) knockin mice were described previously (Fujita et al. 2008). All procedures were performed in accordance with protocols approved by the University of Tokyo Animal Care Committee and the Kanazawa University Animal Care Committee. Experiments were repeated at least three times and gave consistent results.

Plasmids

pCAG-EGFP and pCAG-mCherry were described previously (Sehara et al. 2010). A Foxp2-shRNA-expression vector (Foxp2 shRNA) was constructed using a pSUPER.basic vector (Oligoengine, Seattle, WA) as described previously (Hoshiba et al. in press). The sequences used for shRNA experiments were designed using the web-based software siDIRECT (http://sidirect2.rnai.jp/) and are 5'- GCAGTTAACACTTAATGAA-3' against Foxp2, and 5'-CAACAAGATGAAGAGCACC-3' as non-targeting negative control.

Plasmids were purified using an Endofree plasmid Maxi kit (Qiagen, Germany). Prior to electroporation experiments, plasmid DNA was diluted to 1 mg/mL in TE, and Fast Green solution was added at a final concentration of 0.03% to monitor the injection.

In utero *electroporation*

In utero electroporation was performed as described previously (Fukuchi-Shimogori and Grove 2001; Saito 2006; Tabata and Nakajima 2008; Sehara et al. 2010; Kawasaki et al. 2012) with slight modifications. Briefly, pregnant ICR mice were anesthetized with sodium pentobarbital, and the uterine horns were exposed. Approximately 1–2 µl of DNA solution (1 mg/mL) was injected into the third ventricle of embryos at the indicated ages using a pulled glass micropipette. Each embryo within its uterus was placed between tweezer-type electrodes (CUY650 P0.5-3, NEPA Gene). Square electric pulses (30 V, 50 ms) were passed five times at 1 s intervals using an electroporator (ECM830, BTX). Care was taken to quickly place embryos back into the abdominal cavity to avoid excessive temperature loss. The wall and skin of the abdominal cavity were sutured, and embryos were allowed to develop normally.

In situ *hybridization*

In situ hybridization using digoxigenin-labeled RNA probes was performed as described

previously (Kawasaki et al. 2004; Toda et al. 2013). Briefly, sections prepared from fresh-frozen tissues were treated with 4% paraformaldehyde (PFA) in phosphate-buffered saline (PBS), and 0.25% acetic anhydride in triethanolamine (TEA). The sections were incubated overnight with digoxigenin-labeled RNA probes in hybridization buffer (50% formamide, 5× saline-sodium citrate buffer, 5× Denhardt's solution, 0.3 mg/mL yeast RNA, 0.1 mg/mL herring sperm DNA, and 1 mM dithiothreitol). The sections were then incubated with an alkaline phosphatase-conjugated anti-digoxigenin antibody (Roche) and were visualized using NBT/BCIP as substrates. In some experiments, the sections were then subjected to Hoechst 33342 staining and immunohistochemistry.

Probes used here were mouse *cadherin-6, Foxp2, calbindin 2, Lhx2, Gbx2* and *EphA8*. *Cadherin-6* and *Foxp2* probes were described previously (Iwai et al. 2013; Wakimoto et al. 2015). *Netrin-G1* probe was a generous gift from Dr. Itohara (Nakashiba et al. 2000). *Calbindin 2* and *Lhx2* cDNA fragments were purchased from RIKEN. *Gbx2* and *EphA8* cDNA fragments were amplified by RT-PCR and inserted into pBluescript vectors. The sequences of primers used to amplify *Gbx2*, *EphA8*, *Gad1* and *VGLUT2* cDNA fragments were GAGTCAAAGGTGGAAGATGACC / ACTGCTCTGCACTCAACTCAAA, CCTAGAGTGACAGAGGTCAGGC / CCCTGTTTTCCTGTTGAATAGC, AGCTGATGGCATCTTCCACTCCT / GACTGTGTTCTGAGGTGAAGAGG, and CTGTGGCAGTTGTCACGTTATGC / GCACAGGACACCAGACAGATCAA, respectively.

Immunohistochemistry

Immunohistochemistry was performed as described previously with slight modifications (Kawasaki et al. 2000; Sehara et al. 2010). Sections prepared from fresh-frozen tissues were fixed with 4% PFA/PBS, permeabilized with 0.1-0.5% Triton X-100/PBS, and incubated overnight

with primary antibodies, which included rabbit anti-FOXP2 (Abcam), rabbit anti-FOXP2 (ATLAS), goat anti-FOXP2 (Abcam), rabbit anti-active caspase-3 (Pharmingen), rabbit anti-phospho-histone H3 (PHH3) (Millipore) and rabbit anti-VGLUT2 (Synaptic Systems) antibodies. After incubation with secondary antibodies and Hoechst 33342, the sections were washed and mounted. Sections prepared from perfused tissues were also used. In some experiments, the sections were then subjected to fluorescent Nissl (Molecular Probes) and Hoechst 33342 staining. Epifluorescence microscopy was carried out with an Axioimager A1 microscope (Carl Zeiss, Germany) and a BZ-9000 microscope (KEYENCE, Japan). Confocal microscopy was performed with a FLUOVIEW FV10i (Olympus, Japan). Stereomicroscopy was performed with a MZ16F fluorescence stereomicroscope (Leica, Germany).

DiI tracing

To retrogradely label the soma of thalamic neurons projecting to the prefrontal cortex, P6 pups were anesthetized by cooling, and 0.1 µl of 10% DiI (D3911, Molecular Probes) in dimethylformamide (DMF) was injected into the prefrontal cortex with capillary micropipettes hooked up to a Hamilton 1 µL syringe (Islam et al. 2009). The pups were then perfused with 4% PFA at P7. Brains were isolated and fixed in 4% PFA overnight, and 50 µm sections were cut using a vibratome. The sections were subjected to Hoechst 33342 staining and immunohistochemistry. When sections were labeled with DiI, 1 mg/mL digitonin was used for permeabilization instead of Triton-X 100 because DiI signals tend to be better preserved after 1 mg/mL digitonin treatment than after Triton-X 100 treatment (Matsubayashi et al. 2008).

To retrogradely label the soma of thalamic neurons projecting to the primary somatosensory area (S1) of the cerebral cortex, P13 pups were anesthetized, and 0.1 µl of 10% DiI in DMF was injected into S1 with capillary micropipettes hooked up to a Hamilton 1 µL

syringe (Islam et al. 2009). The pups were then perfused with 4% PFA at P15. Brains were isolated and fixed in 4% PFA overnight, and 50 μm sections were cut using a vibratome. The sections were subjected to Hoechst 33342 staining and to immunohistochemistry using digitonin.

Quantification of the expression levels of Foxp2 immunohistochemistry

Averaged densitometric scans were performed on three adjacent horizontal sections of the embryonic mouse thalamic primordium along the anterior-posterior axis of the thalamus. Briefly, images of Foxp2 immunohistochemistry were digitally acquired with a CCD camera (AxioCam, Zeiss). Using ImageJ software, background signal intensities were subtracted from the images using the rolling ball filter with a diameter of 200 pixels, and the images were then normalized so that each pixel value fell between 0 and 255. Densitometric profiles of Foxp2 signals within rectangular areas along the anterior-posterior axis of the thalamic primordium were generated using the line profile function of ImageJ.

To quantify the percentages of Foxp2-positive cells in the thalamic primordium, horizontal sections of 14 μm thickness were stained with anti-FOXP2 antibody and Hoechst 33342, and *Z*-stack confocal images with 1.6 μm optical thickness were taken. The background signal intensities were defined as the averaged signal intensities of Foxp2-negative cells in the pretectum. After background signal intensity was subtracted from each image, the number of Hoechst-positive cells with Foxp2 immunoreactivity was counted and was divided by the number of Hoechst-positive cells.

To quantify the expression levels of Foxp2 at a single cell level, horizontal sections of 14 μm thickness were stained with anti-FOXP2 antibody and Hoechst 33342, and confocal microscopic images with 1.6 μm optical thickness were analyzed using ImageJ software (National Institutes of Health). For each image, after background signal intensity was subtracted,

the Foxp2 signal intensity in each Hoechst-positive nucleus in the thalamic primordium was measured.

Quantification of the sizes of thalamic nuclei

Coronal sections of 25 μm thickness were prepared from wild type and Foxp2 (R552H) knockin mice at P2, and *in situ* hybridization was performed to visualize thalamic nuclei. The VP and the Pf were identified by the expression patterns of *cadherin-6* and *EphA8*, respectively. The intermediate region of the thalamus was identified by *Lhx2* expression patterns. Images were taken using a Leica stereomicroscope and analyzed using ImageJ software (National Institute of Health).

To quantify the size of the VP, coronal sections located more posterior to the section with the largest LGN were selected. Among these sections, the section containing the largest size of the VP was used for quantification. The periphery of the VP labeled with *cadherin-6* was extracted manually and blindly, and the area of the VP was measured.

To quantify the size of the Pf, coronal sections located more posterior to the section with the largest LGN were selected. Among these sections, the section containing the largest size of the Pf was used for quantification. The periphery of the Pf labeled with *EphA8* was extracted manually and blindly, and the area of the Pf was measured.

To quantify the size of the intermediate region of the thalamus, the section located 200 – 250 μm posterior to the section with the largest LGN was used. The periphery of the intermediate region labeled with *Lhx2* was extracted manually and blindly, and the area of the intermediate region was measured.

Quantification of the number of PHH3-positive cells

To quantify the number of PHH3-positive cells in the thalamic primordium, horizontal sections of 14 μm thickness at E14 were stained with anti-PHH3 antibody and Hoechst 33342. In each section, the number of PHH3-positive cells in the intermediate region of the thalamic primordium was counted blindly and manually.

Results

The expression pattern of Foxp2 in the thalamic primordium of the mouse embryo

It was reported that thalamic nuclei cannot be clearly discerned at embryonic day 12.5 (E12.5) but become distinguishable by E16.5 (Nakagawa and O'Leary 2001). We therefore examined the expression pattern of Foxp2 protein in horizontal sections of the thalamic primordium at E14 using immunohistochemistry (Fig. 1*A*). We used anti-FOXP2 antibody whose specificity we had previously confirmed (Iwai et al. 2013) and found a graded expression pattern of Foxp2 protein in the thalamic primordium (Fig. 1*B*). Foxp2 protein expression levels were highest in the posterior region (Fig. 1*B*, arrowhead), lower in the intermediate region, and lowest in the anterior region of the thalamic primordium (Fig. 1*B*). Consistently, our quantification showed gradual changes in the expression levels of Foxp2 protein in the thalamic primordium (Fig. 1*G*). Immunohistochemistry using another anti-FOXP2 antibody gave similar graded expression patterns in the thalamic primordium (Supplementary Fig. 1*A*). Sagittal sections also showed a graded expression pattern of Foxp2 protein (Fig. 1*D*,*E*). We next examined the expression pattern of *Foxp2* mRNA using *in situ* hybridization. Consistent with the expression pattern of Foxp2 protein, *Foxp2* mRNA was abundant in the posterior region (Fig. 1*C*,*F*, arrowheads) and almost absent in the anterior region of the thalamic primordium (Fig. 1*C*,*F*), which was consistent with a

recent report examining the mRNA expression patterns of various molecules in the developing thalamus (Suzuki-Hirano et al. 2011).

This graded expression pattern of Foxp2 protein in the thalamic primordium could be explained by two possible mechanisms. The first possibility was that the expression level of Foxp2 protein in each cell was indeed low in the anterior region and high in the posterior region. Alternatively, it was also possible that the number of Foxp2-positive cells was smaller in the anterior region than in the posterior region, and as a result, Foxp2 protein expression levels appeared lower in the anterior region macroscopically. To distinguish between these two possibilities, we quantified the percentage of Hoechst-positive cells with Foxp2 immunoreactivity in the thalamic primordium at E14. We found that most cells were Foxp2-positive in both anterior and posterior regions of the thalamic primordium (Fig. 1*I*), suggesting that Foxp2 signal intensity in each cell, rather than the number of Foxp2-positive cells, was lower in the anterior region of the thalamic primordium. Consistently, when we quantified the expression levels of Foxp2 protein at the level of single cells, we found that Foxp2 immunoreactivity in each cell in the anterior region was indeed significantly lower than that in the posterior region of the thalamic primordium (Fig. 1*H,J,K*). We therefore concluded that the expression levels of Foxp2 protein in the anterior region are lower than those in the posterior region of the thalamic primordium. These results indicate that Foxp2 protein has a graded expression pattern in the thalamic primordium during embryonic development, and that the graded expression of Foxp2 protein is achieved, at least partially, at the level of mRNA because graded expression patterns of *Foxp2* mRNA were also detected by *in situ* hybridization (Fig. 1*C,F*).

We next examined the expression patterns of Foxp2 protein in the developing thalamus at different time points. Horizontal sections of the thalamic primordium at E12, E16 and P2 were stained with anti-FOXP2 antibody. Similar to sections at E14, sections at E12 showed

graded expression patterns in the thalamic primordium (Supplementary Fig. 1*B*). In contrast, at E16 and P2, when thalamic nuclei have been already established, the graded expression pattern of Foxp2 protein in the thalamus was lost, and Foxp2 expression remained in some thalamic nuclei (Supplementary Fig. 1*B*). These results suggest that graded expression patterns are present when thalamic patterning proceeds.

The role of Foxp2 in thalamic patterning during development

The graded expression pattern of Foxp2 led us to hypothesize that Foxp2 plays an important role in thalamic patterning during development. To examine the role of Foxp2 in thalamic patterning, we utilized Foxp2 (R552H) knockin mice that have a missense loss-of-function mutation in the forkhead domain of Foxp2 (Fujita et al. 2008; Groszer et al. 2008). This mutation corresponds to a human FOXP2 (R553H) mutation in human FOXP2, and disrupts the DNA binding and transactivation properties of FOXP2 protein (Vernes et al. 2006; Nelson et al. 2013). We conducted VGLUT2 immunohistochemistry using horizontal sections of the thalamus of Foxp2 (R552H) knockin mice at postnatal day 7 (P7) (Fig. 2*A*). We found that the VP of the thalamus, which was reported to express VGLUT2 (Nakamura et al. 2005), was markedly smaller in Foxp2 (R552H) knockin mice than in wild-type control mice (Fig. 2*B*, arrowheads), suggesting that Foxp2 is required for the formation of the VP during development.

Because the VP is located in the posterior region of the thalamus, it seemed plausible that Foxp2 is important for the formation of not only the VP but also other thalamic nuclei located in the posterior region of the thalamus. We examined the expression patterns of molecular markers that are expressed in specific subsets of nuclei in the thalamus, including *EphA8*, *calbindin 2* and *cadherin-6*, using coronal sections (Fig. 2*C*). *EphA8*, *calbindin 2* and *cadherin-6* are expressed in the parafascicular nucleus (Pf), the posterior nucleus (Po) and the VP,

respectively, in the posterior region of the thalamus (Jones and Rubenstein 2004; Yuge et al. 2010; Haddad-Tovolli et al. 2012) (Fig. 2*C*, blue nuclei). We found that *EphA8*- and *calbindin 2*-positive areas were markedly smaller in the posterior region of the thalamus in Foxp2 (R552H) knockin mice (Figs. 2*D* and 3*A*, arrows), suggesting that Foxp2 is required for the formation of the Pf and the Po. *Cadherin-6*-positive areas were also strikingly smaller in Foxp2 (R552H) knockin mice (Figs. 2*D* and 3*A*, arrows), suggesting that Foxp2 is also required for the formation of the VP. This finding is consistent with the result obtained by VGLUT2 immunostaining (Fig. 2*A*,*B*). Quantification of the sizes of thalamic nuclei confirmed that the VP and the Pf were significantly smaller in Foxp2 (R552H) knockin mice (Fig. 2*G*). These results suggest that Foxp2 is important for the formation of thalamic nuclei located in the posterior region of the thalamus.

Given that thalamic nuclei in the posterior region were smaller in Foxp2 (R552H) knockin mice, it seemed possible that those thalamic nuclei changed their identities to different thalamic nuclei. We therefore examined the distribution patterns of markers expressed in the intermediate region of the thalamus, such as *Gbx2* and *Lhx2*, at P2 (Nakagawa and O'Leary 2001; Jones and Rubenstein 2004) (Fig. 2*C*, yellow nuclei). As expected, we found that *Gbx2*- and *Lhx2*-positive areas were markedly larger in Foxp2 (R552H) knockin mice than in wild-type mice (Figs. 2*E* and 3*A*), suggesting that thalamic nuclei in the intermediate region of the thalamus were expanded in Foxp2 (R552H) knockin mice. Quantification also showed that the intermediate region was significantly larger in Foxp2 (R552H) knockin mice (Fig. 2*G*). In contrast, markers of the anterior region of the thalamus (Fig. 2*C*, red nuclei) were not affected in Foxp2 (R552H) knockin mice (Fig. 2*F*). These results suggest that the posterior region of the thalamus obtained the properties of the intermediate region. Taken together, these results indicate that Foxp2 regulates fate determination in the thalamus during development. We also examined the expression patterns of thalamic markers at an earlier stage. Consistent with our results at P2,

cadherin-6-positive areas were markedly smaller in the posterior region of the thalamus (Fig. 3*B*, arrows), and *Gbx2*-positive areas were markedly larger in Foxp2 (R552H) knockin mice at E14 (Fig. 3*B*, arrowheads). This result suggests that thalamic patterning is already affected in Foxp2 (R552H) knockin mice as early as E14.

In addition to the expression patterns of molecular markers, it seemed possible that cytoarchitectonic structures of thalamic nuclei were also affected in Foxp2 (R552H) knockin mice. We therefore conducted Nissl staining using coronal sections of the thalamus of Foxp2 (R552H) knockin mice at P7 (Fig. 2*I*). We found that borders between thalamic nuclei in the thalamus of Foxp2 (R552H) knockin mice were obscure compared with those of wild type mice (Fig. 2*I*). These results suggest that Foxp2 regulates not only the expression patterns of molecular markers but also the formation of cytoarchitectonic structures of thalamic nuclei.

Our results suggest that thalamic patterning is affected in Foxp2 (R552H) knockin mice, but it remained possible that the development of the thalamus itself is abnormal in Foxp2 (R552H) knockin mice, and thalamic patterning within the thalamus is affected secondarily. We found that the expression patterns of *VGLUT2* and *netrin-G1*, which are expressed in the thalamus, were comparable between wild type and Foxp2 (R552H) knockin mice (Fig. 2*H*). Based on these results, the development of the thalamus itself appears to be normal in Foxp2 (R552H) knockin mice. Consistently, the expression of *Gad1*, which is strongly expressed in the prethalamus, was also normal (Fig. 2*H*).

Foxp2 in the thalamus regulates thalamic patterning autonomously

Foxp2 is expressed not only in the thalamus but also in other brain regions such as the cerebral cortex and the striatum (Supplementary Fig. 2). Because we used Foxp2 (R552H) global knockin mice for the analysis of thalamic patterning, it remained possible that changes in thalamic

patterning were mediated by Foxp2 expressed in the other brain regions. To examine the role of Foxp2 in the thalamus, we selectively suppressed Foxp2 expression in the thalamus by introducing a Foxp2-shRNA-expression vector (Foxp2 shRNA) into the thalamus using *in utero* electroporation at E11.0 (Fig. 4*A*). Foxp2 immunohistochemistry showed that the Foxp2 shRNA effectively suppressed Foxp2 expression in the thalamus at E14 (Fig. 4*B*, arrowheads). To examine if introducing Foxp2 shRNA into the thalamic primordium affects thalamic patterning, coronal sections of the thalamus were prepared at E18, and the expression patterns of molecular markers of thalamic nuclei were examined using *in situ* hybridization. Consistent with the results obtained with Foxp2 (R552H) knockin mice, the introduction of Foxp2 shRNA into the thalamic primordium suppressed the expression of *EphA8* and *cadherin-6* (Fig. 4*C*, arrowheads) and increased that of *Gbx2* and *Lhx2* (Fig. 4*D*, arrows), suggesting that Foxp2 shRNA reduced the size of the posterior region of the thalamus but increased that of the intermediate region of the thalamus. These results suggest that Foxp2 expressed in the thalamus regulates thalamic patterning.

It remained possible that Foxp2 regulates not only thalamic patterning but also apoptosis and/or proliferation in the thalamus. We stained horizontal sections of the thalamic primordium with anti-active caspase-3 antibody at E14 and found only a few active caspase-3-positive cells in the thalamic primordium (Supplementary Fig. 3*A*), suggesting that apoptosis is not involved in the phenotype of Foxp2 (R552H) knockin mice. We also stained horizontal sections of the thalamic primordium with anti-phospho-histone H3 (PHH3) antibody at E14. There were no statistically significant differences in the number of PHH3-positive cells in the intermediate region of the thalamic primordium between wild type and Foxp2 (R552H) knockin mice (wild type 26.6 ± 10.8 cells/section, Foxp2 (R552H) 36.6 ± 4.9 cells/section; P = 0.21; Student's t-test, mean ± SD) (Supplementary Fig. 3*B*), suggesting that cell proliferation is

not affected in Foxp2 (R552H) knockin mice.

Foxp2 regulates thalamocortical projection patterns

To examine if Foxp2 regulates not only gene expression patterns in the thalamus but also thalamocortical projection patterns, we used the neuronal tracer DiI (Fig. 5*A*). Because the intermediate region of the thalamus projects to the prefrontal cortex (Conde et al. 1995; Hoover and Vertes 2007) and was expanded in Foxp2 (R552H) knockin mice (Fig. 2), we injected DiI into the prefrontal cortex at P6 and examined if retrogradely labeled DiI-positive areas in the thalamus would be expanded in Foxp2 (R552H) knockin mice (Fig. 5*A*). One day after DiI injection, we made coronal sections of the cerebral cortex and confirmed that DiI was indeed injected into the prefrontal cortex (Fig. 5*B*,*C*). Then, coronal sections of the thalamus were stained with anti-VGLUT2 antibody using digitonin, which is a detergent suitable for DiI-labeled sections (Matsubayashi et al. 2008). As expected, we found that DiI-positive retrogradely labeled areas were much larger in Foxp2 (R552H) knockin mice than in wild-type mice (Fig. 5*D*, arrows). This expanded DiI-positive area corresponded to the expanded *Gbx2*-positive intermediate region of the thalamus (Fig. 5*E*, arrowheads). These results suggest that Foxp2 regulates not only gene expression patterns in the thalamus but also thalamocortical projection patterns.

To examine whether thalamocortical projections from the Po are decreased in Foxp2 (R552H) knockin mice, we injected DiI into S1, where thalamocortical axons from both the VP and the Po were observed in wild type mice (Fig. 5*F*). Two days after DiI injection, we made coronal sections of the cerebral cortex and confirmed that the DiI-injected area was located within S1, which had VGLUT2-positive barrels (Fig. 5*G*, arrows). We then made coronal sections of the thalamus and examined the distribution patterns of retrogradely labeled DiI-positive soma in the thalamus. The sections were stained with anti-VGLUT2 antibody, which strongly recognizes the

VB (Fig. 5*H*, asterisks) but only faintly recognizes the Po (Fig. 5*H*, arrows) (Fremeau et al. 2001; Nakamura et al. 2005). As expected, DiI-positive soma existed in both the VP (Fig. 5*H*, asterisks) and the Po (Fig. 5*H*, arrows) in wild type mice. In contrast, we found that DiI-positive retrogradely labeled soma were present in the VB of Foxp2 (R552H) knockin mice (Fig. 5*H*, asterisks), they were almost absent in the Po (Fig. 5*H*, arrowheads). This result suggests that thalamocortical projections from the Po are reduced in S1 of Foxp2 (R552H) knockin mice. Taken together with the results of our experiments involving molecular markers, these results indicate that the Po was almost absent in Foxp2 (R552H) knockin mice.

As we have shown, the VP was smaller in Foxp2 (R552H) knockin mice (Fig. 2). Because the VP contains whisker-related patterns called barreloids (Van Der Loos 1976), we thought it would be intriguing to examine if barreloid patterns in the VP were affected in Foxp2 (R552H) knockin mice. Coronal sections of the thalamus were subjected to VGLUT2 immunostaining at P7. We found that barreloid patterns were severely disrupted in Foxp2 (R552H) knockin mice (Fig. 6*A*, arrow). The disrupted barreloid patterns in the thalamus led us to examine barrel patterns in S1 of the cerebral cortex using VGLUT2 immunostaining. We found that barrel patterns were lost in the anterior portion of the postero-medial barrel subfield (PMBSF), the antero-lateral barrel subfield (ALBSF) and the region of S1 corresponding to the forelimb (Fig. 6*B*, arrowheads). This is consistent with the idea that disruption of barreloid patterns in the thalamus leads to disruption of barrel patterns in the cerebral cortex.

We have also shown that the Po in the thalamus was lost in Foxp2 (R552H) knockin mice (Fig. 2). The Po sends thalamocortical axons to septa (Alloway 2008; Sehara and Kawasaki 2011), which are the areas between barrels in layer 4 of S1 in the cerebral cortex. We therefore hypothesized that thalamocortical projections from the Po were decreased, and septa were shrunken in Foxp2 (R552H) knockin mice. Consistent with our hypothesis, VGLUT2

immunostaining of S1 showed that VGLUT2-negative areas between VGLUT2-positive barrels were narrower in Foxp2 (R552H) knockin mice than in wild-type mice (Fig. 6*B*, inset, arrows).

Discussion

We have shown that Foxp2 has a graded expression pattern in the thalamic primordium during development. In Foxp2 (R552H) knockin mice, thalamic nuclei in the posterior region of the thalamus were shrunken, while those in the intermediate region were expanded (Fig. 6*C*). Our findings indicate that Foxp2 is crucial for thalamic development.

Foxp2 is a transcription factor regulating thalamic patterning

Although transcription factors distinguishing the thalamic primordium from adjacent brain structures such as the prethalamus, the pretectum and the epithalamus during development have been intensively investigated (Kiecker and Lumsden 2012), transcription factors that regulate patterning inside the thalamus are still largely unclear. Our results suggest that Foxp2 is crucial for determining the identities of thalamic nuclei. Previously, the transcription factor Gbx2 was reported to be important for thalamic development. It was reported that Gbx2 suppressed neuronal cell death in a specific subset of thalamic nuclei, and Gbx2 knockout resulted in abnormal arrangements of thalamic nuclei (Szabo et al. 2009). These results indicate that Foxp2 and Gbx2 play distinct roles in thalamic development. In addition, we also found that thalamic nuclei in the anterior region of the thalamus were not affected in Foxp2 (R552H) knockin mice, raising the possibility that the identities of the anterior region are determined by other transcription factors. Uncovering additional transcription factors regulating thalamic patterning

would be an important goal for future experiments.

Previous pioneering studies have demonstrated that both the antero-posterior components and the medio-lateral components are correlated with thalamo-cortical projection patterns (Molnar et al. 1998; Vanderhaeghen and Polleux 2004; Molnar et al. 2012). Our findings indicate that Foxp2 mediates thalamic patterning along the antero-posterior axis. To understand the entire picture of thalamic patterning during development, it would be intriguing to uncover the mechanisms regulating the medio-lateral components of thalamic patterning. In addition, in this paper, we investigated the role of Foxp2 in thalamocortical projections postnatally. Therefore, the following two possibilities remain to explain the changes in thalamocortical projections of Foxp2 (R552H) knockin mice. The first possibility is thalamocortical projections are altered from early in development in Foxp2 (R552H) knockin mice. The other is that thalamocortical projections are formed normally at the beginning, and then turn out to be affected postnatally in Foxp2 (R552H) knockin mice. Because our experiments showed that molecular markers were affected in the embryos of Foxp2 (R552H) knockin mice, the former seems likely, but it would be important to address this issue.

Molecular mechanisms downstream of Foxp2 in thalamic development

To understand the entire picture of the mechanisms underlying thalamic development, including thalamic patterning and thalamocortical projections, uncovering the molecular mechanisms downstream of Foxp2 would be important.

It would be intriguing to investigate whether the molecules that mediate the formation of borders between distinct nuclei in other systems are located downstream of Foxp2 in the thalamus. While Foxp2 has a continuous graded expression pattern in the thalamic primordium early in development, discrete domains of each thalamic nucleus are formed later. It seems

plausible that the mechanisms downstream of Foxp2 convert areas along this continuous gradient into distinct domains of thalamic nuclei. A similar conversion has been well studied in the developing spinal cord (Briscoe and Ericson 2001; Dessaud et al. 2008). Transcription factors expressed in two adjacent areas in the developing spinal cord comprise a cross-repressive interaction and delineate boundaries between them (Ericson et al. 1997; Briscoe et al. 1999). Similar mechanisms could be located downstream of Foxp2.

The expression of axon guidance molecules could be regulated by Foxp2 because thalamocortical projection patterns are affected in Foxp2 (R552H) knockin mice. Although it has been established that ephrin and netrin-1 signaling molecules regulate thalamocortical projection patterns (Dufour et al. 2003; Powell et al. 2008), the regulatory mechanisms upstream of these axon guidance molecules are still largely unclear. It seems likely that Foxp2 regulates the expressions of the ephrin and/or netrin family member molecules.

Recently, lists of candidate molecules that could play important roles downstream of Foxp2 have been identified (Spiteri et al. 2007; Vernes et al. 2007; Fujita et al. 2008; Vernes et al. 2011). Although these molecules were identified using brain regions other than the thalamus, they seem to be attractive candidate molecules that could mediate the effects of Foxp2 in thalamic development. Interestingly, the expression level of the transcription factor Lhx2, which is expressed in the developing thalamus, was found to be regulated by Foxp2 in the cerebellum. Lhx2 could mediate thalamic patterning downstream of Foxp2. Combining our data and the findings reported in the previous literature could guide future experiments toward uncovering the entire picture of the patterning of the thalamus.

Roles of Foxp2 during development

The roles of Foxp2 have been intensively investigated in brain regions other than the thalamus.

For example, knockdown of Foxp2 resulted in reduced spine density in Area X of the zebra finch, suggesting that Foxp2 regulates spine dynamics (Schulz et al. 2010). Foxp2 (R552H) knockin mice showed deficits in motor-skill learning, accompanied by abnormal synaptic plasticity in striatal and cerebellar neural circuits, suggesting that Foxp2 is crucial for synaptic plasticity (Groszer et al. 2008). Foxp2 knockout resulted in an absence of ultrasonic vocalization in mouse pups, suggesting a role of Foxp2 in social communication functions (Shu et al. 2005; Fujita et al. 2008). Abnormalities of neuronal morphology were observed in mice with disruptions in Foxp2 (Shu et al. 2005; Fujita et al. 2008). During development, it was reported that Foxp2 increased neuronal differentiation in the embryonic forebrain and regulated neurite outgrowth in primary neurons (Vernes et al. 2011; Chiu et al. 2014). Our results uncovered an additional role of Foxp2, which is as a regulator of neuronal patterning during development.

One attractive hypothesis is that FOXP2 is involved in the acquisition of language during evolution. Indeed, FOXP2 is mutated in a monogenic syndrome causing speech and language dysfunction (Lai et al. 2001). Furthermore, two amino acid substitutions in the mouse Foxp2 allele, which are found in humans, caused alterations in corticobasal ganglia circuits, indicating that humanized Foxp2 has different functions from mouse Foxp2 (Enard et al. 2009; Reimers-Kipping et al. 2011). Combined with the fact that the thalamic nucleus pulvinar, which is located in the posterior region of the thalamus and is related to perceptual confidence, is observed only in carnivores and primates (Butler 2007; Komura et al. 2013), our finding raised the possibility that the appearance of the pulvinar during evolution was determined by Foxp2. It would be intriguing to examine if mice with humanized Foxp2 have a thalamic structure similar to the pulvinar.

Funding

This work was supported by the Global Centers of Excellence program and the Grant-in-Aid for Scientific Research from the Ministry of Education, Culture, Sports, Science and Technology-Japan; Takeda Science Foundation. This work was also supported by a Research Fellowship for Young Scientists from Japan Society for the Promotion of Science; the Teijin-Kumura scholarship (to H. E.).

Notes

We are grateful to Drs. S. Tsuji, T. Kadowaki, H. Bito (The University of Tokyo), E. Nishida (Kyoto University), the late Y. Sasai, and S. Nakanishi for their warm support, and Dr. S. Itohara (RIKEN) for plasmids. We thank K. Tanno, Y. Ichikawa and Mr. Osugi for their assistance and Z. Blalock for discussions. We also thank all the Kawasaki lab members for their support.

Conflict of Interest: None declared.

References

Alloway KD. 2008. Information processing streams in rodent barrel cortex: the differential functions of barrel and septal circuits. Cereb Cortex. 18:979-989.

Bluske KK, Vue TY, Kawakami Y, Taketo MM, Yoshikawa K, Johnson JE, Nakagawa Y. 2012. beta-Catenin signaling specifies progenitor cell identity in parallel with Shh signaling in the developing mammalian thalamus. Development. 139:2692-2702.

Braun MM, Etheridge A, Bernard A, Robertson CP, Roelink H. 2003. Wnt signaling is required at distinct stages of development for the induction of the posterior forebrain. Development. 130:5579-5587.

Briscoe J, Ericson J. 2001. Specification of neuronal fates in the ventral neural tube. Curr Opin Neurobiol. 11:43-49.

Briscoe J, Sussel L, Serup P, Hartigan-O'Connor D, Jessell TM, Rubenstein JL, Ericson J. 1999. Homeobox gene Nkx2.2 and specification of neuronal identity by graded Sonic hedgehog signalling. Nature. 398:622-627.

Butler AB. 2007. The dual elaboration hypothesis of the evolution of the dorsal thalamus. In: Kaas JH, editor. Evolution of Nervous Systems. San Diego (CA): Academic Press. p 517-523.

Chatterjee M, Guo Q, Weber S, Scholpp S, Li JY. 2014. Pax6 regulates the formation of the habenular nuclei by controlling the temporospatial expression of Shh in the diencephalon in vertebrates. BMC Biol. 12:13.

Chiu YC, Li MY, Liu YH, Ding JY, Yu JY, Wang TW. 2014. Foxp2 regulates neuronal differentiation and neuronal subtype specification. Dev Neurobiol. 74:723-738.

Conde F, Maire-Lepoivre E, Audinat E, Crepel F. 1995. Afferent connections of the medial frontal cortex of the rat. II. Cortical and subcortical afferents. J Comp Neurol. 352:567-593.

Dessaud E, McMahon AP, Briscoe J. 2008. Pattern formation in the vertebrate neural tube: a sonic hedgehog morphogen-regulated transcriptional network. Development. 135:2489-2503.

Dufour A, Seibt J, Passante L, Depaepe V, Ciossek T, Frisen J, Kullander K, Flanagan JG, Polleux F, Vanderhaeghen P. 2003. Area specificity and topography of thalamocortical projections are controlled by ephrin/Eph genes. Neuron. 39:453-465.

Enard W, Gehre S, Hammerschmidt K, Holter SM, Blass T, Somel M, Bruckner MK, Schreiweis C, Winter C, Sohr R et al. 2009. A humanized version of Foxp2 affects cortico-basal ganglia circuits in mice. Cell. 137:961-971.

Ericson J, Rashbass P, Schedl A, Brenner-Morton S, Kawakami A, van Heyningen V, Jessell TM, Briscoe J. 1997. Pax6 controls progenitor cell identity and neuronal fate in response to graded Shh signaling. Cell. 90:169-180.

Fisher SE, Scharff C. 2009. FOXP2 as a molecular window into speech and language. Trends Genet. 25:166-177.

Fremeau RT, Jr., Troyer MD, Pahner I, Nygaard GO, Tran CH, Reimer RJ, Bellocchio EE,

Fortin D, Storm-Mathisen J, Edwards RH. 2001. The expression of vesicular glutamate transporters defines two classes of excitatory synapse. Neuron. 31:247-260.

French CA, Jin X, Campbell TG, Gerfen E, Groszer M, Fisher SE, Costa RM. 2012. An aetiological Foxp2 mutation causes aberrant striatal activity and alters plasticity during skill learning. Mol Psychiatry. 17:1077-1085.

Fujita E, Tanabe Y, Shiota A, Ueda M, Suwa K, Momoi MY, Momoi T. 2008. Ultrasonic vocalization impairment of Foxp2 (R552H) knockin mice related to speech-language disorder and abnormality of Purkinje cells. Proc Natl Acad Sci U S A. 105:3117-3122.

Fukuchi-Shimogori T, Grove EA. 2001. Neocortex patterning by the secreted signaling molecule FGF8. Science. 294:1071-1074.

Groszer M, Keays DA, Deacon RM, de Bono JP, Prasad-Mulcare S, Gaub S, Baum MG, French CA, Nicod J, Coventry JA et al. 2008. Impaired synaptic plasticity and motor learning in mice with a point mutation implicated in human speech deficits. Curr Biol. 18:354-362.

Haddad-Tovolli R, Heide M, Zhou X, Blaess S, Alvarez-Bolado G. 2012. Mouse thalamic differentiation: gli-dependent pattern and gli-independent prepattern. Front Neurosci. 6:27.

Hannenhalli S, Kaestner KH. 2009. The evolution of Fox genes and their role in development and disease. Nat Rev Genet. 10:233-240.

Hirata T, Nakazawa M, Muraoka O, Nakayama R, Suda Y, Hibi M. 2006. Zinc-finger genes Fez

and Fez-like function in the establishment of diencephalon subdivisions. Development. 133:3993-4004.

Hoover WB, Vertes RP. 2007. Anatomical analysis of afferent projections to the medial prefrontal cortex in the rat. Brain Struct Funct. 212:149-179.

Hoshiba Y, Toda T, Ebisu H, Wakimoto M, Yanagi S, Kawasaki H. in press. Sox11 balances dendritic morphogenesis with neuronal migration in the developing cerebral cortex. J Neurosci.

Islam SM, Shinmyo Y, Okafuji T, Su Y, Naser IB, Ahmed G, Zhang S, Chen S, Ohta K, Kiyonari H et al. 2009. Draxin, a repulsive guidance protein for spinal cord and forebrain commissures. Science. 323:388-393.

Iwai L, Ohashi Y, van der List D, Usrey WM, Miyashita Y, Kawasaki H. 2013. FoxP2 is a parvocellular-specific transcription factor in the visual thalamus of monkeys and ferrets. Cereb Cortex. 23:2204-2212.

Jones EG. 2007. The human thalamus. In: Jones EG, editor. The Thalamus. 2 ed. New York (NY): Cambridge University Press. p 1396-1450.

Jones EG, Rubenstein JL. 2004. Expression of regulatory genes during differentiation of thalamic nuclei in mouse and monkey. J Comp Neurol. 477:55-80.

Kawasaki H, Crowley JC, Livesey FJ, Katz LC. 2004. Molecular organization of the ferret visual thalamus. J Neurosci. 24:9962-9970.

Kawasaki H, Iwai L, Tanno K. 2012. Rapid and efficient genetic manipulation of gyrencephalic carnivores using in utero electroporation. Mol Brain. 5:24.

Kawasaki H, Mizuseki K, Nishikawa S, Kaneko S, Kuwana Y, Nakanishi S, Nishikawa SI, Sasai Y. 2000. Induction of midbrain dopaminergic neurons from ES cells by stromal cell-derived inducing activity. Neuron. 28:31-40.

Kiecker C, Lumsden A. 2012. The role of organizers in patterning the nervous system. Annu Rev Neurosci. 35:347-367.

Kobayashi D, Kobayashi M, Matsumoto K, Ogura T, Nakafuku M, Shimamura K. 2002. Early subdivisions in the neural plate define distinct competence for inductive signals. Development. 129:83-93.

Komura Y, Nikkuni A, Hirashima N, Uetake T, Miyamoto A. 2013. Responses of pulvinar neurons reflect a subject's confidence in visual categorization. Nat Neurosci. 16:749-755.

Lai CS, Fisher SE, Hurst JA, Vargha-Khadem F, Monaco AP. 2001. A forkhead-domain gene is mutated in a severe speech and language disorder. Nature. 413:519-523.

Lehmann OJ, Sowden JC, Carlsson P, Jordan T, Bhattacharya SS. 2003. Fox's in development and disease. Trends Genet. 19:339-344.

Matsubayashi Y, Iwai L, Kawasaki H. 2008. Fluorescent double-labeling with carbocyanine neuronal tracing and immunohistochemistry using a cholesterol-specific detergent digitonin. J Neurosci Methods. 174:71-81.

Molnar Z, Adams R, Blakemore C. 1998. Mechanisms underlying the early establishment of thalamocortical connections in the rat. J Neurosci. 18:5723-5745.

Molnar Z, Garel S, Lopez-Bendito G, Maness P, Price DJ. 2012. Mechanisms controlling the guidance of thalamocortical axons through the embryonic forebrain. Eur J Neurosci. 35:1573-1585.

Nakagawa Y, O'Leary DD. 2001. Combinatorial expression patterns of LIM-homeodomain and other regulatory genes parcellate developing thalamus. J Neurosci. 21:2711-2725.

Nakagawa Y, O'Leary DD. 2003. Dynamic patterned expression of orphan nuclear receptor genes RORalpha and RORbeta in developing mouse forebrain. Dev Neurosci. 25:234-244.

Nakamura K, Hioki H, Fujiyama F, Kaneko T. 2005. Postnatal changes of vesicular glutamate transporter (VGluT)1 and VGluT2 immunoreactivities and their colocalization in the mouse forebrain. J Comp Neurol. 492:263-288.

Nakashiba T, Ikeda T, Nishimura S, Tashiro K, Honjo T, Culotti JG, Itohara S. 2000. Netrin-G1: a novel glycosyl phosphatidylinositol-linked mammalian netrin that is functionally divergent from classical netrins. J Neurosci. 20:6540-6550.

Nelson CS, Fuller CK, Fordyce PM, Greninger AL, Li H, DeRisi JL. 2013. Microfluidic affinity and ChIP-seq analyses converge on a conserved FOXP2-binding motif in chimp and human, which enables the detection of evolutionarily novel targets. Nucleic Acids Res. 41:5991-6004.

Peukert D, Weber S, Lumsden A, Scholpp S. 2011. Lhx2 and Lhx9 determine neuronal differentiation and compartition in the caudal forebrain by regulating Wnt signaling. PLoS Biol. 9:e1001218.

Powell AW, Sassa T, Wu Y, Tessier-Lavigne M, Polleux F. 2008. Topography of thalamic projections requires attractive and repulsive functions of Netrin-1 in the ventral telencephalon. PLoS Biol. 6:e116.

Puelles E, Acampora D, Gogoi R, Tuorto F, Papalia A, Guillemot F, Ang SL, Simeone A. 2006. Otx2 controls identity and fate of glutamatergic progenitors of the thalamus by repressing GABAergic differentiation. J Neurosci. 26:5955-5964.

Reimers-Kipping S, Hevers W, Paabo S, Enard W. 2011. Humanized Foxp2 specifically affects cortico-basal ganglia circuits. Neuroscience. 175:75-84.

Robertshaw E, Matsumoto K, Lumsden A, Kiecker C. 2013. Irx3 and Pax6 establish differential competence for Shh-mediated induction of GABAergic and glutamatergic neurons of the thalamus. Proc Natl Acad Sci U S A. 110:E3919-3926.

Saito T. 2006. In vivo electroporation in the embryonic mouse central nervous system. Nat Protoc. 1:1552-1558.

Schulz SB, Haesler S, Scharff C, Rochefort C. 2010. Knockdown of FoxP2 alters spine density in Area X of the zebra finch. Genes Brain Behav. 9:732-740.

Sehara K, Kawasaki H. 2011. Neuronal circuits with whisker-related patterns. Mol Neurobiol. 43:155-162.

Sehara K, Toda T, Iwai L, Wakimoto M, Tanno K, Matsubayashi Y, Kawasaki H. 2010. Whisker-related axonal patterns and plasticity of layer 2/3 neurons in the mouse barrel cortex. J Neurosci. 30:3082-3092.

Shu W, Cho JY, Jiang Y, Zhang M, Weisz D, Elder GA, Schmeidler J, De Gasperi R, Sosa MA, Rabidou D et al. 2005. Altered ultrasonic vocalization in mice with a disruption in the Foxp2 gene. Proc Natl Acad Sci U S A. 102:9643-9648.

Spiteri E, Konopka G, Coppola G, Bomar J, Oldham M, Ou J, Vernes SC, Fisher SE, Ren B, Geschwind DH. 2007. Identification of the transcriptional targets of FOXP2, a gene linked to speech and language, in developing human brain. Am J Hum Genet. 81:1144-1157.

Suzuki-Hirano A, Ogawa M, Kataoka A, Yoshida AC, Itoh D, Ueno M, Blackshaw S, Shimogori T. 2011. Dynamic spatiotemporal gene expression in embryonic mouse thalamus. J Comp Neurol. 519:528-543.

Szabo NE, Zhao T, Zhou X, Alvarez-Bolado G. 2009. The role of Sonic hedgehog of neural origin in thalamic differentiation in the mouse. J Neurosci. 29:2453-2466.

Tabata H, Nakajima K. 2008. Labeling embryonic mouse central nervous system cells by in utero electroporation. Dev Growth Differ. 50:507-511.

Toda T, Homma D, Tokuoka H, Hayakawa I, Sugimoto Y, Ichinose H, Kawasaki H. 2013. Birth regulates the initiation of sensory map formation through serotonin signaling. Dev Cell. 27:32-46.

Van Der Loos H. 1976. Barreloids in mouse somatosensory thalamus. Neurosci Lett. 2:1-6.

Vanderhaeghen P, Polleux F. 2004. Developmental mechanisms patterning thalamocortical projections: intrinsic, extrinsic and in between. Trends Neurosci. 27:384-391.

Vernes SC, Nicod J, Elahi FM, Coventry JA, Kenny N, Coupe AM, Bird LE, Davies KE, Fisher SE. 2006. Functional genetic analysis of mutations implicated in a human speech and language disorder. Hum Mol Genet. 15:3154-3167.

Vernes SC, Oliver PL, Spiteri E, Lockstone HE, Puliyadi R, Taylor JM, Ho J, Mombereau C, Brewer A, Lowy E et al. 2011. Foxp2 regulates gene networks implicated in neurite outgrowth in the developing brain. PLoS Genet. 7:e1002145.

Vernes SC, Spiteri E, Nicod J, Groszer M, Taylor JM, Davies KE, Geschwind DH, Fisher SE. 2007. High-throughput analysis of promoter occupancy reveals direct neural targets of FOXP2, a gene mutated in speech and language disorders. Am J Hum Genet. 81:1232-1250.

Wakimoto M, Sehara K, Ebisu H, Hoshiba Y, Tsunoda S, Ichikawa Y, Kawasaki H. 2015. Classic Cadherins Mediate Selective Intracortical Circuit Formation in the Mouse Neocortex. Cereb Cortex. 25:3535-3546.

Yuge K, Kataoka A, Yoshida AC, Itoh D, Aggarwal M, Mori S, Blackshaw S, Shimogori T. 2010. Region-specific gene expression in early postnatal mouse thalamus. J Comp Neurol. 519:544-561.

Figure legends

Figure 1. Expression patterns of Foxp2 in the thalamic primordium of the mouse embryo.

(*A*) Schematic organization of horizontal sections of the embryonic mouse brain. Images within the box are shown in (*B*) and (*C*). Ctx, cerebral cortex; Th, thalamic primordium. (*B*) Foxp2 immunohistochemistry using horizontal sections of mouse thalamic primordium at E14. The areas within the broken lines are the thalamic primordium. Note that Foxp2 protein was abundantly expressed in the posterior region (arrowhead) but almost absent in the anterior region of the thalamic primordium. (*C*) *In situ* hybridization using horizontal sections of mouse thalamic primordium at E14. *Foxp2* mRNA was also abundantly expressed in the posterior region of the thalamic primordium (arrowhead). (*D*) Schematic organization of sagittal sections of the embryonic mouse brain. Images within the box are shown in (*E*) and (*F*). Ctx, cerebral cortex; Th, thalamic primordium. (*E*) Foxp2 immunohistochemistry using sagittal sections of mouse thalamic primordium at E14. The areas within the broken lines are the thalamic primordium. (*F*) *In situ* hybridization using sagittal sections of mouse thalamic primordium at E14. *Foxp2* mRNA was abundantly expressed in the posterior region of the thalamic primordium (arrowhead). (*G*) A representative densitometry scan along the anterior (A) to posterior (P) axis of the thalamic primordium in horizontal sections at E14. (*H*) Higher-magnification images of Foxp2 immunohistochemistry of the thalamic primordium. (*I*) The percentages of Foxp2-positive cells. The numbers of Foxp2-positive cells in the anterior region (A) and the posterior region (P) were counted and divided by those of Hoechst-positive cells. Note that most cells have Foxp2 immunoreactivity in both anterior and posterior regions. An error bar indicates SD. (*J*) Foxp2 immunoreactivity in each cell was measured, and the averages in the anterior region (A) and the posterior region (P) of the thalamic primordium are shown. The expression level of Foxp2 in the

anterior region was significantly lower than that in the posterior region. * $P < 0.05$, Welch's *t*-test. Error bars indicate SEM. (*K*) Histogram of Foxp2 immunoreactivity in each cell in the anterior region and the posterior region of the thalamic primordium. Note that most cells in the anterior region had very low Foxp2 expression levels. A, anterior; P, posterior; L, lateral; M, medial; D, dorsal; V, ventral. Scale bars = 250 μm (*B, C, E, F*) and 20 μm (*H).*

Figure 2. The identities of thalamic nuclei of Foxp2 (R552H) knockin mice.

(*A*) Schematic organization of horizontal sections of the mouse brain at P7. Images within the box are shown in (*B*). Ctx, cerebral cortex; Th, Thalamus; Cb, cerebellum. (*B*) VGLUT2 immunohistochemistry using horizontal sections of the thalamus of Foxp2 (R552H) knockin mice at P7. The ventral posterior nucleus (VP) in the thalamus was smaller in Foxp2 (R552H) knockin mice (arrowheads). A, anterior; P, posterior. AD, the anterodorsal nucleus; AV, the anteroventral nucleus; VP, the ventral posterior nucleus. (*C*) Schematic organization of coronal sections of the mouse brain. Coronal sections were prepared from Foxp2 (R552H) knockin mice at P2, and were examined using *in situ* hybridization. Marker expressions in the thalamic nuclei are shown in the upper right panel. Images within the box of the lower left panel are shown in (*D*), (*E*) and (*F*). Ctx, cerebral cortex; Th, thalamus. A, anterior; P, posterior; D, dorsal; V, ventral. (*D*) The posterior region of the thalamus. *EphA8* is expressed in the parafascicular nucleus (Pf), and *calbindin 2* (*Calb2*) is expressed in the posterior nucleus (Po). *Cadherin-6* (*Cad6*) is expressed in the VP. Note that the Pf, the Po, and the VP were markedly smaller in Foxp2 (R552H) knockin mice (arrows). (*E*) The intermediate region of the thalamus. *Lhx2* is expressed in the central lateral nucleus (CL), and *Gbx2* is expressed in the CL and the mediodorsal nucleus (MD). Note that the CL and the MD were larger in Foxp2 (R552H) knockin mice (arrows). (*F*) The anterior region of the thalamus. *Cadherin-6* (*Cad6*) is expressed in the anterodorsal nucleus (AD), the

anteroventral nucleus (AV) and the reticular nucleus (Rt). *Calbindin 2* (*Calb2*) is expressed in the lateral dorsal nucleus (LD). The sizes of the AD, the AV, the Rt and the LD were unaffected (arrows). (*G*) Quantitative analyses of the effects of Foxp2 (R552H) on the sizes of thalamic nuclei. The sizes of the *cadherin-6* (*Cad6*)-positive area in (*D*) (VP), the *EphA8*-positive area in (*D*) (Pf), and the *Lhx2*-positive area in (*E*) (Intermediate) were measured. The VB and the Pf were significantly smaller, and the intermediate region was significantly larger in Foxp2 (R552H) knockin mice. * $P < 0.01$, two-sided Student's *t*-test. Error bars indicate SD. (*H*) Coronal sections were prepared at P2 and were examined using *in situ* hybridization. The expression patterns of *VGLUT2, netrin-G1* and *Gad1* were not affected in Foxp2 (R552H) knockin mice. (*I*) Coronal sections of the thalamus at P7 were subject to Nissl staining. In control mice, thalamic nuclei were well segregated, and borders between thalamic nuclei were clearly visible (arrows). In contrast, borders between thalamic nuclei became obscure in Foxp2 (R552H) knockin mice. Scale bars = 1 mm (*B,D-F,H* and *I*)

Figure 3. The changes of thalamic nuclei in horizontal sections of Foxp2 (R552H) knockin mice.

(*A*) Horizontal sections of the thalamus were prepared from Foxp2 (R552H) knockin mice at P2, and were examined using *in situ* hybridization. Note that the *Lhx2*-positive area was expanded posteriorly in Foxp2 (R552H) knockin mice (square brackets), while *EphA8*- and *cadherin-6 (Cad6)*-positive areas were shrunken (arrows). (*B*) Horizontal sections of the thalamus were prepared at E14 and were examined using *in situ* hybridization. Note that the *Gbx2*-positive area is larger at the posterior region of the thalamic primordium in Foxp2 (R552H) knockin mice (arrowheads), while the *cadherin-6* (*Cad6*)-positive area is shrunken in Foxp2 (R552H) knockin mice (arrows). A, anterior; P, posterior. Scale bars = 2 mm (*A*) and 200 μm (*B*).

Figure 4. Foxp2 knockdown in the thalamus changed thalamic patterning.

(*A*) Top: Experimental procedure of *in utero* electroporation to investigate the role of Foxp2 within the thalamus. pCAG-mCherry (0.2 mg/mL) and pSUPER-Foxp2-shRNA (0.8 mg/mL) were co-transfected into the thalamic primordium using *in utero* electroporation at E11.0, and coronal sections were prepared at E14 and E18. Bottom: Schematic organization of coronal sections of the embryonic mouse brain. Images within the box are shown in (*C*) and (*D*). Ctx, cerebral cortex; Th, thalamus. D, dorsal; V, ventral. (*B*) Foxp2 immunostaining at E14. Note that Foxp2 immunoreactivity was markedly suppressed by Foxp2 shRNA (arrowheads). (*C*) Expression patterns of *EphA8* and *cadherin-6* (*Cad6*) visualized with *in situ* hybridization. Note that the expression of *EphA8* and *cadherin-6* was suppressed by Foxp2 shRNA (arrowheads). (*D*) Expression patterns of *Gbx2* and *Lhx2* visualized with *in situ* hybridization. Note that *Gbx2*- and *Lhx2*-negative areas (arrows) became *Gbx2*- and *Lhx2*-positive in the Foxp2 shRNA-transfected thalamus. Scale bars = 50 μm (*B*) and 500 μm (*C, D)*.

Figure 5. Thalamocortical projections in Foxp2 (R552H) knockin mice.

(*A*) Experimental design. Thalamic neurons projecting to the prefrontal cortex were retrogradely labeled with DiI. DiI was injected into the prefrontal cortex at P6, and coronal sections were prepared at P7. (*B*) Dorsal views of DiI-injected brains. DiI-injected areas are indicated by arrows. (*C*) Coronal sections of the prefrontal cortex. The injection sites of DiI solutions were visible (arrows). (*D*) Coronal sections of the thalamus stained with anti-VGLUT2 antibody. Thalamic neurons projecting to the prefrontal cortex were retrogradely labeled with DiI. Note that many DiI-positive neurons were observed in Foxp2 (R552H) knockin mice (arrows). (*E*) Coronal sections of the thalamus of Foxp2 (R552H) knockin mice were prepared. After images of the DiI signal were taken, *in situ* hybridization was conducted with a *Gbx2* probe using the same sections. Note that the expanded DiI-positive area was *Gbx2*-positive (arrowheads). (*F*)

Experimental design. To retrogradely label thalamic neurons projecting to S1, DiI was injected into S1 at P13, and sections were prepared at P15. (*G*) Coronal sections of DiI-injected cortical areas stained with anti-VGLUT2 antibody. Note that the DiI-positive area was located within S1, which has barrels (arrowheads). (*H*) Coronal sections of the thalamus stained with anti-VGLUT2 antibody, which strongly labeled the VP (asterisks). The VP was retrogradely labeled with DiI both in control and Foxp2 (R552H) knockin mice (asterisks), suggesting that DiI was successfully injected into S1. Note that DiI signal in the Po of wild type mice (arrows) was lost in Foxp2 (R552H) knockin mice (arrowheads). Scale bars = 3 mm (*B*), 1 mm (*C*), 500 μm (*D*), 200 μm (*E*), 200 μm (*G*), and 400 μm (*H*).

Figure 6. Abnormal organization of barreloids in the thalamus and barrels in the cerebral cortex.

(*A*) Coronal sections of the thalamus were prepared at P7 and stained with anti-VGLUT2 antibody to visualize whisker-related patterns of barreloids in the VP of the thalamus. While barreloids were well segregated in control mice, they were disrupted in Foxp2 (R552H) knockin mice (arrow). (*B*) Tangential sections were prepared from the flattened cerebral cortex and were stained with anti-VGLUT2 antibody to visualize barrel patterns in S1. While barrel patterns were clearly visible in control mice, clear barrel patterns were lost in the majority of S1 in Foxp2 (R552H) knockin mice (arrowheads). Magnified images are shown in the insets. Note that VGLUT2-negative septa (arrows) are narrower in Foxp2 (R552H) knockin mice. (*C*) Schematic organization of coronal sections of the thalamus in wild type and Foxp2 (R552H) knockin mice. Thalamic nuclei in the posterior region of the thalamus (blue) are shrunken in Foxp2 (R552H) knockin mice, whereas thalamic nuclei in the intermediate region are expanded (yellow). Thalamic nuclei in the anterior region of the thalamus (red) are not affected in Foxp2 (R552H) knockin mice. A, anterior; P, posterior. Scale bars = 200 μm (*A*), 1 mm (*B*), 200 μm (*B*, inset).

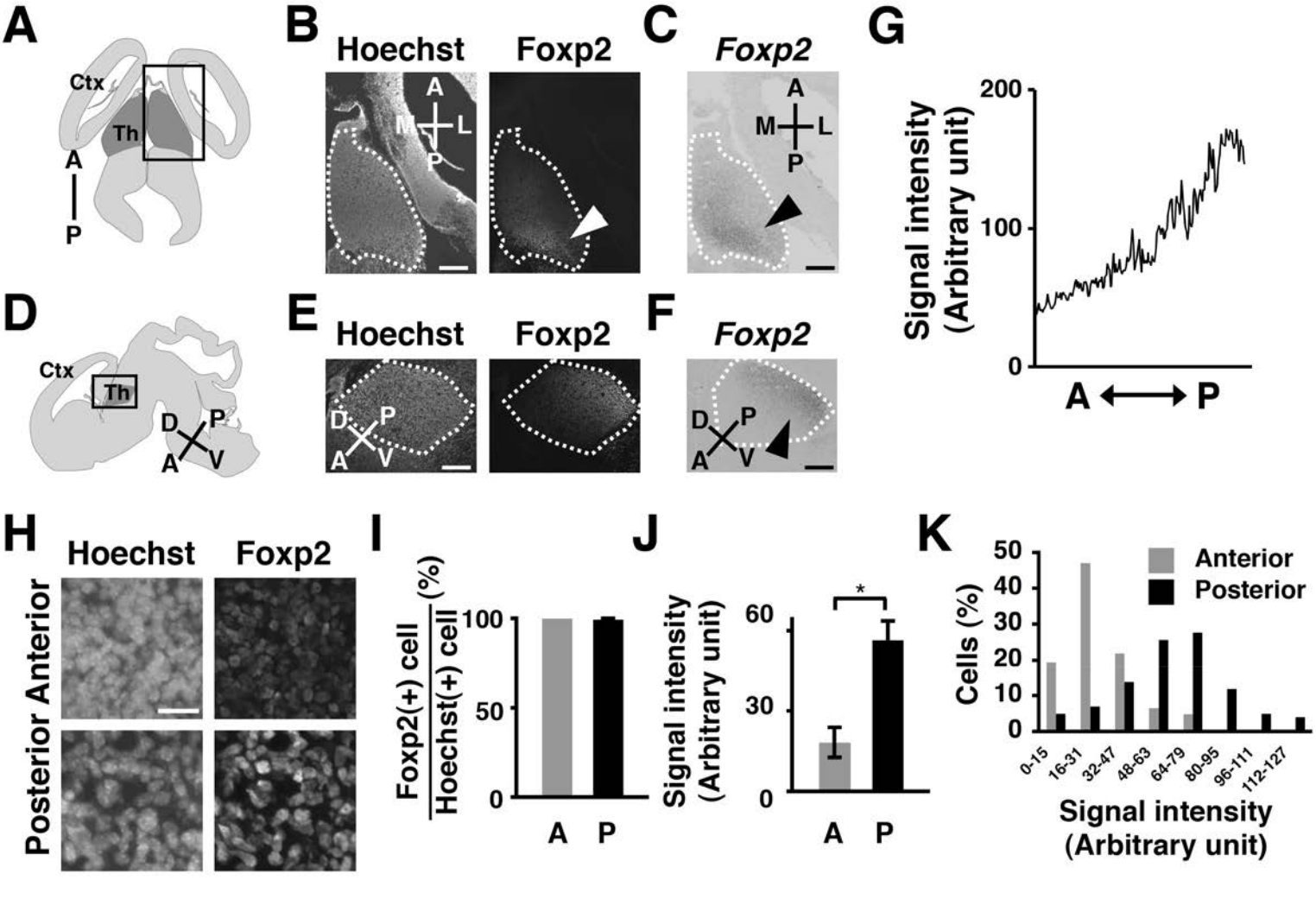
A
Ctx
Th
A
P
B
Hoechst
Foxp2
A
M
L
P
C
Foxp2
A
M
L
P
G
Signal intensity
(Arbitrary unit)
200
100
0
A
P
D
Ctx
Th
D
P
A
V
E
Hoechst
Foxp2
D
P
A
V
F
Foxp2
D
P
A
V
H
Hoechst
Foxp2
Posterior Anterior
I
Foxp2(+) cell
Hoechst(+) cell
(%)
100
50
0
A
P
J
Signal intensity
(Arbitrary unit)
*
60
30
0
A
P
K
Cells (%)
50
40
30
20
10
0
Anterior
Posterior
0-15
16-31
32-47
48-63
64-79
80-95
96-111
112-127
Signal intensity
(Arbitrary unit)

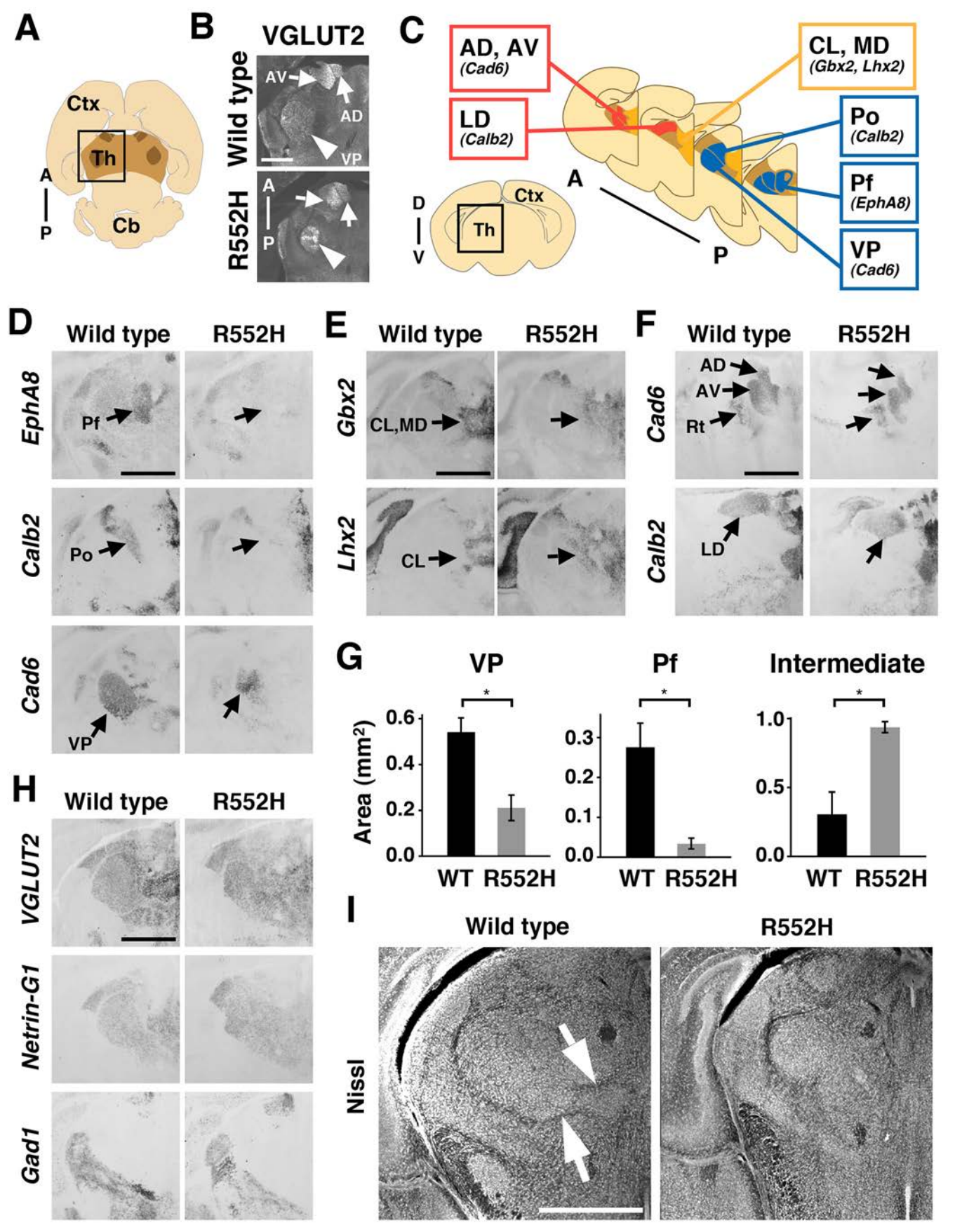
A
Ctx
Th
Cb
A
P
B
VGLUT2
Wild type
R552H
AV
AD
VP
A
P
C
AD, AV
(Cad6)
LD
(Calb2)
CL, MD
(Gbx2, Lhx2)
Po
(Calb2)
Pf
(EphA8)
VP
(Cad6)
D
V
Ctx
Th
A
P
D
Wild type
R552H
EphA8
Pf
Calb2
Po
Cad6
VP
E
Wild type
R552H
Gbx2
CL,MD
Lhx2
CL
F
Wild type
R552H
Cad6
AD
AV
Rt
Calb2
LD
G
VP
Pf
Intermediate
Area (mm²)
0.6
0.4
0.2
0.0
0.3
0.2
0.1
0.0
1.0
0.5
0.0
*
WT
R552H
H
Wild type
R552H
VGLUT2
Netrin-G1
Gad1
I
Wild type
R552H
Nissl

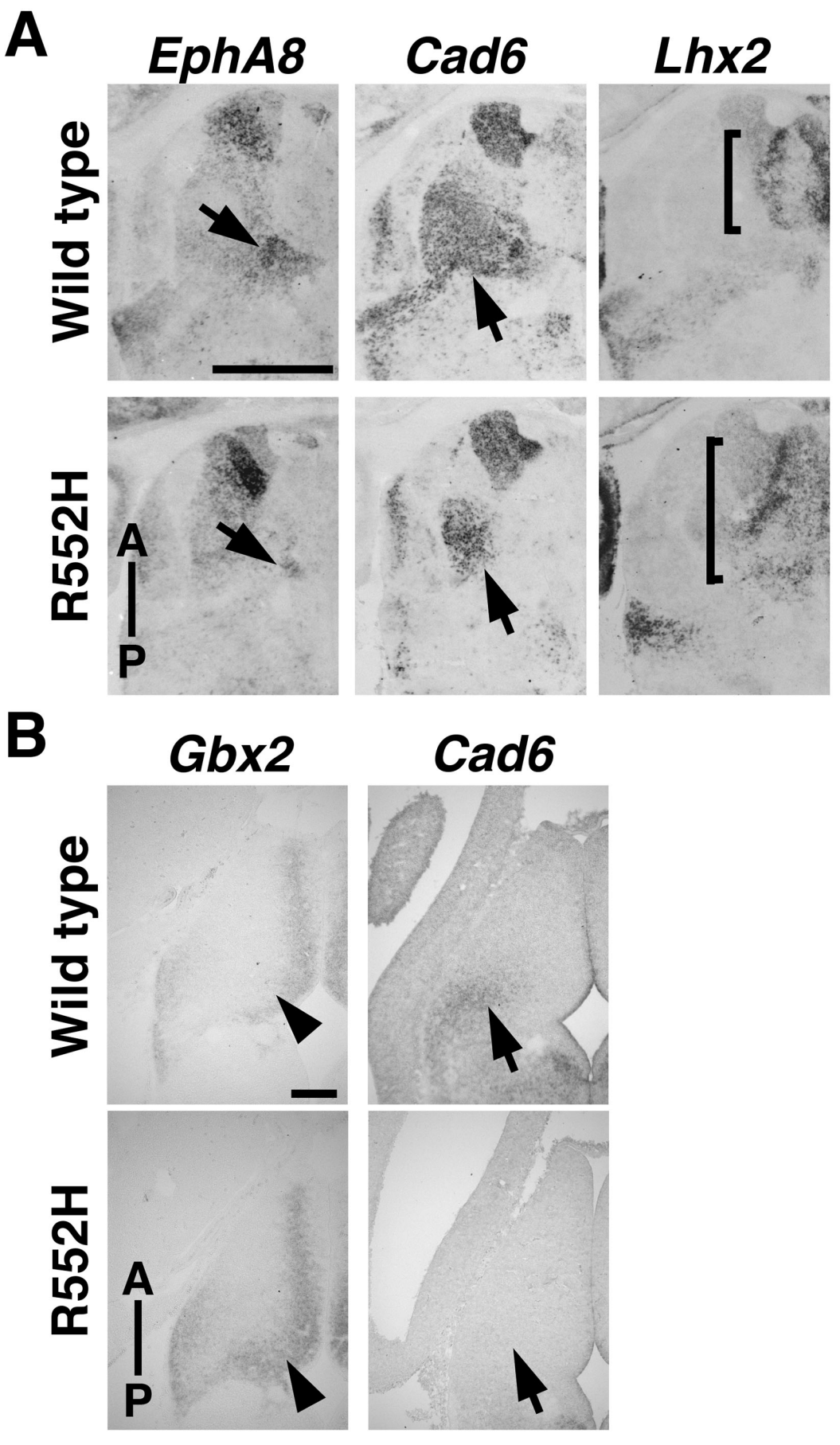
A
EphA8
Cad6
Lhx2
Wild type
R552H
A
P
B
Gbx2
Cad6
Wild type
R552H
A
P

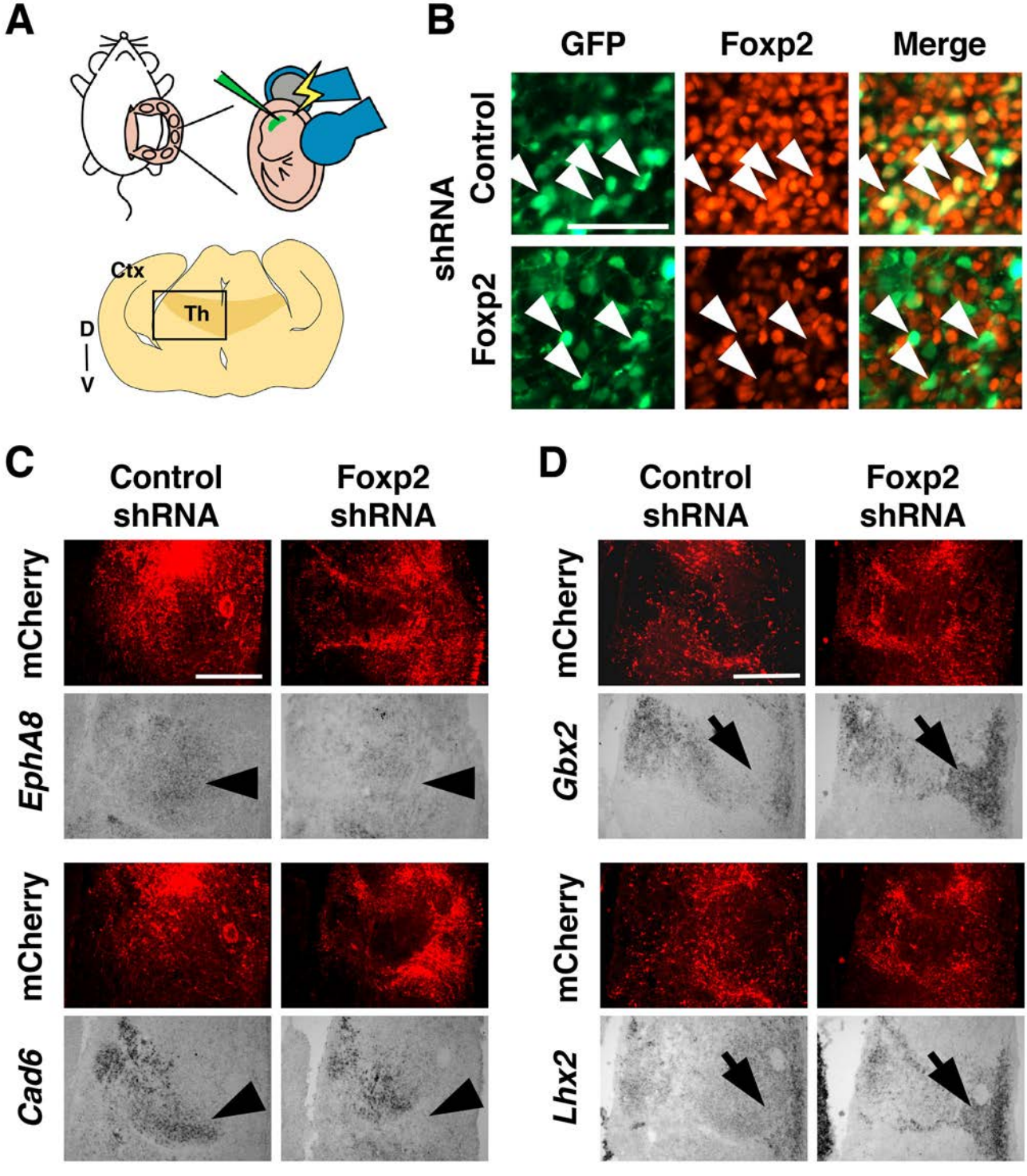
A
Ctx
Th
D
V
B
GFP
Foxp2
Merge
shRNA
Control
Foxp2
C
Control shRNA
Foxp2 shRNA
mCherry
EphA8
mCherry
Cad6
D
Control shRNA
Foxp2 shRNA
mCherry
Gbx2
mCherry
Lhx2

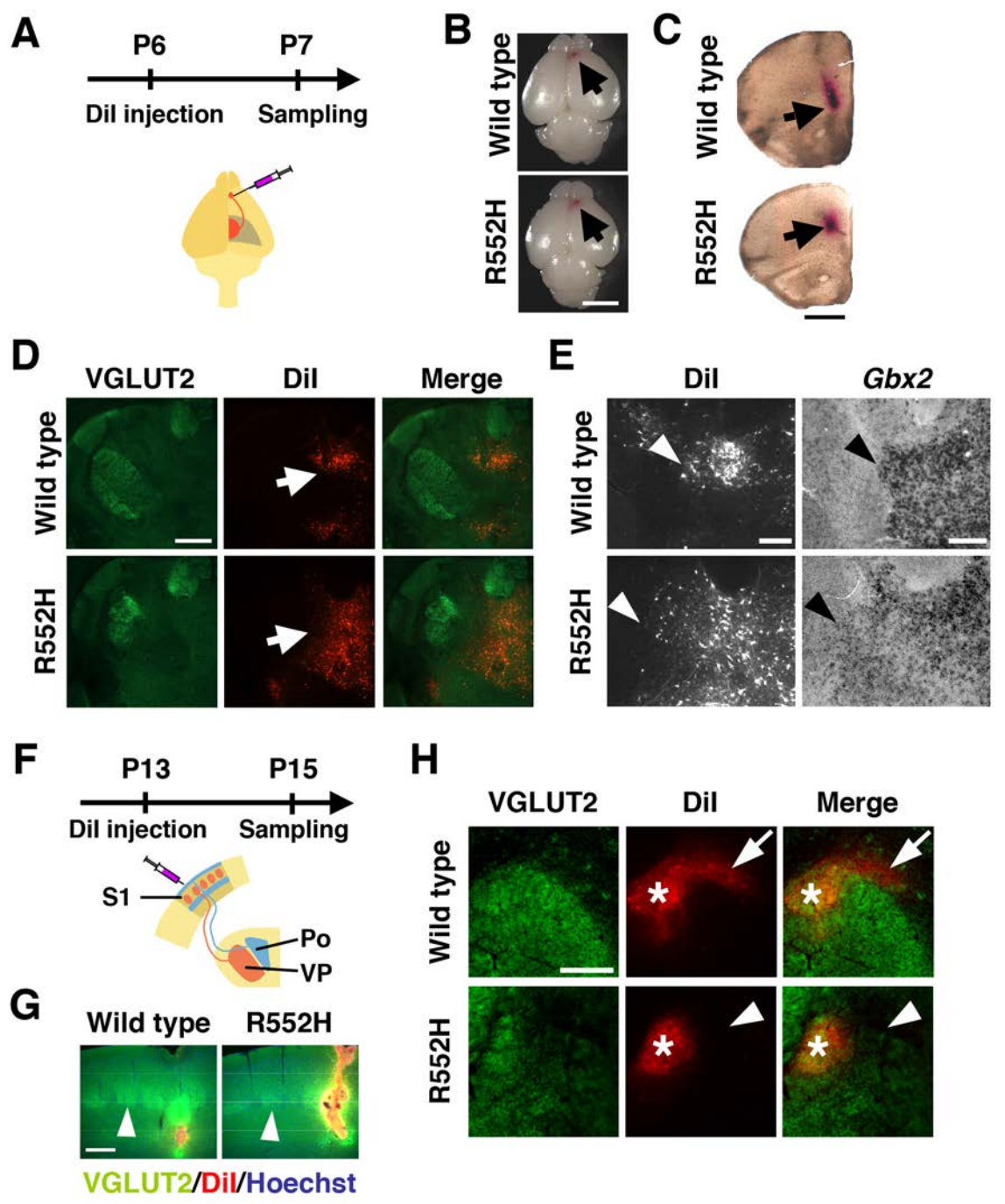
A
P6
P7
DiI injection
Sampling
B
Wild type
R552H
C
Wild type
R552H
D
VGLUT2
DiI
Merge
Wild type
R552H
E
DiI
Gbx2
Wild type
R552H
F
P13
P15
DiI injection
Sampling
S1
Po
VP
G
Wild type
R552H
VGLUT2/DiI/Hoechst
H
VGLUT2
DiI
Merge
Wild type
R552H

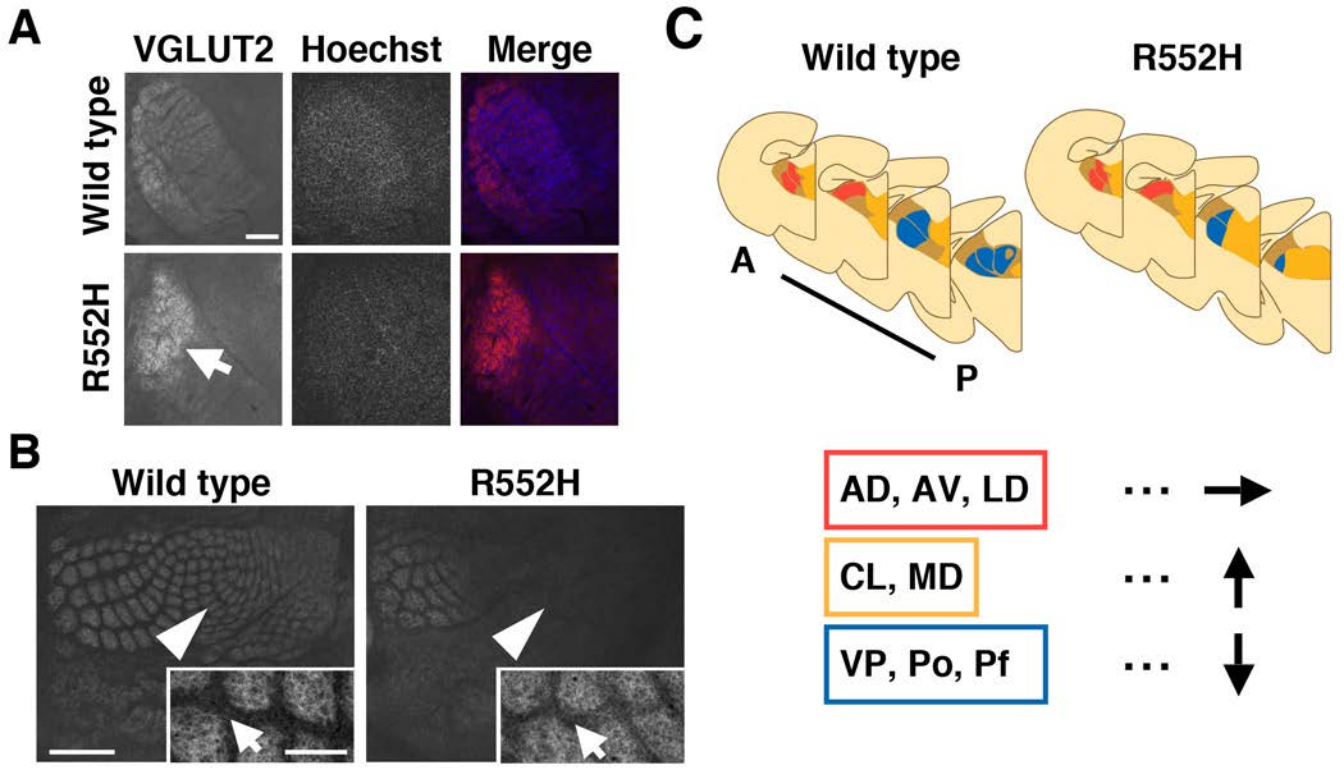
A
VGLUT2
Hoechst
Merge
Wild type
R552H
B
Wild type
R552H
C
Wild type
R552H
A
P
AD, AV, LD
CL, MD
VP, Po, Pf